SUPPLEMENTAL MATERIAL

Gremlin plays a key role in the pathogenesis of pulmonary hypertension.

Edwina Cahill PhD[1], Christine M. Costello PhD[1], Simon C Rowan BSc[1], Susan Harkin[1], Katherine Howell PhD[1], Martin O. Leonard PhD[1], Mark Southwood PhD[3], Eoin P Cummins PhD[1], Susan F Fitzpatrick BSc[1], Cormac Taylor PhD[1], Nicholas W. Morrell MD[3], Finian Martin PhD[2], Paul McLoughlin MB BCh PhD[1,#]

[1]University College Dublin, School of Medicine and Medical Sciences and [2]School of Biomedical and Biomolecular Sciences, Dublin, Ireland and [3]University of Cambridge School of Clinical Medicine, Cambridge, United Kingdom.

[#]Correspondence should be addressed to:

Dr Paul McLoughlin MB BCh PhD.

University College Dublin,

School of Medicine and Medical Sciences,

Belfield, Dublin 4, Ireland.

e-mail.   Paul.mcloughlin@ucd.ie

Phone.   +353 1 716 6583.   Fax.   +353 1 716 6649

Supplemental Methods

Mice. All procedures involving mice were approved by the UCD Animal Research Ethics Sub-Committee and carried out under license from the Department of Health.

Chronic hypoxic pulmonary hypertension was induced by housing male C57BL/6 mice (10-12 weeks) in a hypoxic normobaric opaque perspex environmental chamber ($FiO_2 < 0.10$, $FiCO_2 < 0.01$) and weight-matched normoxic mice were maintained in normoxic conditions in the same room ($FiO_2 = 0.21$, $FiCO_2 < 0.01$). Oxygen concentrations were monitored using an automated gas analyzer (Pro-Ox and Pro-CO_2, Biospherix). The chamber was opened every 1-2 days for approximately 30 minutes to allow for changing of cages and replacement of food and water. Excess CO_2 produced by the mice was removed using a tray of soda lime placed inside the chamber. All mice were maintained in a specific pathogen-free (SPF) facility with free access to water and food.

Gremlin1 heterozygote knockout mice (grem1^{+/-}) were bred and pups genotyped by extracting DNA from ear punches and determining the presence of the LacZ knock-in gene by end-point PCR as described previously[1, 2].

RNA Isolation and real-time PCR. Total RNA was extracted from snap-frozen whole tissue or cells using a Qiagen RNeasy kit (RNeasy Mini Kit, Qiagen) and reverse-transcribed (RT) to cDNA using Superscript II RNase H-Reverse Transcriptase kit (Invitrogen) as previously described[3]. TaqMan real-time PCR was performed using 18S rRNA as the endogenous loading control gene. Reactions were carried out on the ABI PRISM 7900 Sequence Detection System with TaqMan Universal PCR Master Mix and TaqMan Gene Expression Assays (Applied Biosystems). Relative quantification of mRNA expression levels was determined using the standard curve method and normalised to 18S.

Immunohistochemical analysis

To obtain mouse lung sections, male C57BL/6 mice (*n*=5) were maintained in normoxia or exposed to 10% oxygen for two days. The mice were killed by exsanguination under general anesthesia, the lungs removed and then fixed by intratracheal instillation of paraformaldehyde (4%) at standard pressure (25 cm of water). The lungs were then immersed in paraformaldehyde and left overnight, cut into blocks, embedded in paraffin wax and sections (7μm) cut and mounted onto poly-l-lysine-coated glass slides (Sigma-Aldrich). Immunohistochemistry was performed as previously described using goat anti-gremlin antibody (R&D Systems)[3]. No staining was detected when gremlin primary antibody was omitted or substituted with an irrelevant antibody also raised in goat (anti-HAND1, R&D Systems).

Specimens from human lungs with IPAH (*n* = 2) and FPAH (*n* = 2) were obtained at time of transplant while control specimens were obtained from lung tissue resected during surgery for cancer at a site remote from the tumor margins. All patients had provided full written consent. Sections were prepared and immunostained for gremlin as above.

Immunoflourescence Staining

Mouse lungs were fully inflated using paraformaldehyde (1%) for 30mins and then placed into sucrose solutions (30%) at 4˚C for 24 hours before infiltration with OCT compound (Tissue Tek®, Sakura Finetek). Sections (10 microns) were cut and mounted onto poly-L-lysine coated slides for immunostaining and fluorescent labelling using the tyramide signal amplification (TSA™ Biotin System, Perkin Elmer Inc.). Slides were immersed in glycine (100mM) for 45 minutes to quench formaldehyde-induced fluorescence followed by immersion in sodium borohydride

(0.1%) for 30mins. Slides were washed and blocked in TNB blocking buffer (supplied in TSA™ kit) for 30mins, and incubated with anti-gremlin antibody (R&D Systems) overnight at 4°C. Slides were then incubated in biotinylated rabbit anti-goat secondary antibody (Vector Laboratories) for 1 hour, washed, and incubated in streptavidin-HRP (supplied in TSA™ kit) and subsequently biotinyl tyramide amplification reagent (supplied in TSA™ kit). FITC-streptavidin (Sigma-Aldrich) was added for 1 hour. Tissue sections were counterstained with 4',6-diamidino-2-phenylindole (Sigma-Aldrich) and mounted using Vectashield (Vector Laboratories). Images were acquired using a confocal laser-scanning microscope (Zeiss, LSM 510 Meta, x40/NA1.3 and x63/NA1.4 oil immersion objectives). No fluorescence was observed when gremlin primary antibody was omitted.

Western Blotting and ELISA

Western blot analysis was performed using whole lung and cell lysates that were lysed in radioimmuno-precipitation assay (RIPA) buffer supplemented with serine protease inhibitor, phenlyethanesulfonylflouride (PMSF), and a cocktail of protease and phosphatase inhibitors (Sigma-Aldrich). Tissue was homogenised (Ultra-Turrax T8, Carl Stuart) and cells were lysed by repetitive vortexing. Total protein content was determined using the bicinchoninic acid (BCA) assay (Pierce). Cell conditioned medium was concentrated using 5kDa Ultra-15 filters (Millipore) by centrifugation in a swinging bucket rotor (4000g for 45mins at 4°C). Protein extracts were separated by 15% (vol/vol) SDS-PAGE and blotted using: rabbit p-Smad1/5/8 (Cell Signaling Technology), rabbit total Smad1/5/8 (Santa Cruz Biotechnology), goat gremlin (R&D Systems), goat BMPR2 (R&D Systems), rabbit BMP2 and BMP4 (Abcam). These were detected with the respective, species-specific horseradish peroxidise-

conjugated secondary antibodies (Dako and Chemicon). Densitometry was performed using ImageJ software normalising to GAPDH or vehicle.

An Enzyme-Linked Immunosorbent Assay (ELISA) (R&D Systems) was used to examine the presence of secreted BMP ligands in concentrated conditioned medium from HMVEC-L. ELISAs were performed according to the protocols provided by the manufacturer (R&D Systems).

Cell Culture

For *in vitro* studies, primary human pulmonary microvascular endothelial cells from lung (HMVEC-L) and primary smooth muscle cells isolated from human pulmonary artery (PASMC) were bought in from Lonza Bioscience (formerly Cambrex). Cells were grown on sterile tissue culture dishes in Endothelial Growth Medium (EGM-2MV; Code: CC-3202) or Smooth Muscle Growth Medium (SmGM-2; Code CC-3182) according to the manufacturers instructions. All cells used in these experiments were passage 6-7 and were routinely checked for mycoplasma contamination using the VenorGeM PCR kit (Cambio Ltd). For hypoxic experiments, cells were placed in a hypoxic chamber (Coy Labs) and cultured in an atmosphere of $1\% \ O_2$, $5\% \ CO_2$ and $94\% \ N_2$ for 48 hours. Control conditions were achieved by culture in $21\% \ O_2$, $5\% \ CO_2$ and $74\% \ N_2$ in a cell-culture incubator.

To knock-down endogenous HIF1α or HIF2α, cells (HMVEC-L) were transfected with 10nM of a Smartpool HIF1α or HIF2α-specific siRNA respectively (Dharmacon) using lipofectin (Invitrogen Life Technologies). A non-targeting Smartpool siRNA was used as a negative control. Cells were grown on 6 well plates in EGM-2MV medium without antibiotics. When cells were 30-40% confluent, cells were transfected using Optimem reduced-serum media for 4 hours. Following

transfection cells were placed in normoxic or hypoxic (1% O_2) conditions for a further 48 hours. HIF1α and HIF2α mRNA expression levels were measured by Real-Time RT-PCR to confirm effective reduction with specific siRNA. Gremlin 1 expression was also analysed by Real-Time RT-PCR.

For Smad1/5/8 phosphorylation experiments hypoxic serum-free conditioned medium (CM) was taken off cells that were incubated in hypoxia for 48 hours and briefly centrifuged to remove dead cells. For detection of Smad1/5/8 phosphorylation, cells were serum-starved overnight in serum-free medium (SFM) containing supplements and treatments were added the following day for 1 hour as follows: 2 microngrams/ml of recombinant gremlin 1, 80ng/ml of BMP4 or 100ng/ml of BMP2 (all from R&D Systems). To block gremlin 1 antagonizing activity, 15 micrograms/ml of anti-gremlin antibody (R&D Systems) was pre-incubated with hypoxic conditioned medium or recombinant gremlin 1 for 1 hour prior to treatment. In all experiments in which hypoxia conditioned medium was not added unconditioned medium was added instead.

The concentrations of recombinant BMP2 (100ng/ml) and BMP4 (80mn/ml) used were chosen from within the range of concentrations previously reported[4-10]. In pilot experiments, we confirmed that the chosen concentrations accelerated wound healing compared to vehicle but did not cause complete wound closure; thus the effect of any further intervention, which *a priori* might either have reduced or augmented the effect of the BMPs, could be detected.

The concentration of recombinant gremlin used (2mg/ml) was selected based on previously published reports[11,12]. In pilot experiments we confirmed that this concentration blocked BMP2-induced Smad phosphorylation. We then confirmed that we had identified a concentration of gremlin that produced an inhibitory effect on

BMP2-induced Smad phosphorylation and endothelial wound healing similar to that of hypoxia conditioned medium. These findings suggest that the concentration of recombinant gremlin we used produced local concentrations of biologically active gremlin in the endothelial cell microenvironment similar to those produced by hypoxic endothelial cells.

For scratch healing assays HMVEC-L were seeded and allowed to grow to a confluent monolayer and a single vertical scratch was applied to each chamber using a 10-100 microlitre pipette tip (Greiner). Treatments were added in low-serum medium (3%) for 24 hours and percentage wound closure was measured using ImageJ software as previously described[3]. Hypoxia conditioned medium for these experiments was prepared as described above. In all experiments in which hypoxic conditioned medium was not added, unconditioned medium was added instead. Six fields of view in each well were measured at the pre-defined positions (above and below each drawn line) and each experiment was repeated six times.

Assessment of hypoxia-induced changes in pulmonary vascular resistance

Pulmonary hemodynamic responses were assessed using an isolated ventilated lung preparation perfused at constant flow, as previously described[13]. This preparation permits direct assessment of pulmonary vascular resistance independently of alterations in cardiovascular function, reflex, hormonal or other factors changed by chronic hypoxia[14-16]. Wild-type and grem1^{+/-} mice were exposed to hypoxic (F_IO_2=0.10) conditions in a normobarbic environmental chamber or maintained in normoxia (F_IO_2=0.21) in the same room for 3 weeks, as previously described[15]. The hypoxic chamber was opened for 30 minutes every 1-2 days for

changes of water, feed and bedding and removal of mice from, or additon of mice to, the chamber.

Following exposure, mice were then anaesthetised (70mg.kg^{-1} sodium pentobarbitone (Rhône Merieux Ltd, Harlow, UK) intraperitoneally and anti-coagulated (1000 units kg^{-1} heparin). A cannula was then inserted into the trachea via tracheostomy and the mouse ventilated (5% CO_2 in air, tidal volume of 250µl, respiratory frequency 90). The femoral artery was then exposed and the mouse killed by exsanguination. A sample of blood was obtained for measurement of hematocrit. A midline incision was made through the sternum and the ribs retracted to expose the heart and lungs. A cannula was then inserted into the pulmonary artery and left atrium. The lungs were perfused (2ml/min) with DMEM heated to 37°C, pH 7.45 with Ficoll (4 g/100ml, PM 70, Sigma-Aldrich) according to standard protocols[13] and were hyperinflated to an airway pressure of 15cmH$_2$O every 5 minutes. End expiratory pressure was set to 1.6 mmHg and the venous outflow pressure to 2 mmHg. Following stabilization of the preparation, pressure measurements were recorded as the mean of 10 determinations made at end expiration during consecutive breaths, thus ensuring that vascular pressures and resistance were determined in Zone 3 conditions. Measurements were made in the final minute prior to a regular hyperinflation. In a subset of lungs, the rho kinase inhibitor Y27632 (Merck Biosciences) was then added to the perfusate (10^{-5}M) and vascular pressures recorded once the reductions had stabilized[15].

After completion of the perfusion protocol, the hearts were separated from the lungs, fixed by immersion in paraformaldehyde (4%) and stored. The atria were removed at the level of the atrioventricular junction in the plane of the mitral and tricuspid annuli i.e. at the level of the openings of the tricuspid and mitral valves

where the valve leaflets attach. The ventricles were then transected parallel to this plane at two levels, one third and two thirds of the distance from the atrioventricular junction to the apex of the heart. The relative cross sectional areas of the cut surfaces of the right and left ventricles were determined at each of these two levels and the mean of the two results was taken as the value for that heart (RV:LV+S). The cross sectional areas of the cut surfaces of the right and left ventricle were determined by stereological analysis. Images of the cut curfaces were acquired, digitised and viewed under a superimposed stereological grid showing regularly spaced points (Visiopharm integrator system version 2.9.11.0; Olympus Denmark). Points landing on right ventricle and on left ventricle+septum were separately counted and the ratio of these two determined at each level. The mean of these two values was taken as the RV:LV+S for that heart.

Stereological Quantification of Pulmonary Vascular structure

Hypoxia induced changes in pulmonary vascular structure were assessed in separate groups of wild-type and grem1$^{+/-}$ mice exposed to hypoxic or normoxic conditions for 3 weeks. Mice were then anaesthetized (sodium pentobarbitone 70mg.kg^{-1}, Rhône Merieux Ltd) intraperitoneally and anti-coagulated (1000 units kg^{-1} heparin). A midline incision was made through the sternum and the ribs retracted to expose the lungs. Tracheal and pulmonary arterial cannulae were inserted into the pulmonary artery as described above. An incision was made in the apex of the left ventricle to facilitate free drainage of perfusate. Initially rho-kinase inhibitor (Y-27632 10^{-5}M, Merck Biosciences) in normal saline was perfused through the pulmonary circulation to inhibit ROCK activity and ensure complete relaxation of vasomotor tone[15]. Defibrinated horse blood (Cruinn Diagnostics Ltd.) was then perfused

through the vasculature (pulmonary arterial pressure $30 cmH_2O$ above the hilum)

until the pulmonary vessels were uniformly filled. The presence of erthyrocytes in

the vascular space facilitated identification of vessels within the pulmonary

parenchyma following the preparation of sections for microscopic examination.

Horse erythrocytes are of similar size (average diameter 5.8 microns) to mouse red

blood cells (average diameter 6.1 microns)[17]. Once all the blood vessels had been

filled, as indicated by a uniformly red appearance of all lung lobes, the wound at the

apex of the left ventricle was closed using a vascular clamp ensuring that pressure

throughout the vessels was uniform ($30 cmH_2O$). The pulmonary arterial trunk was

then tied closed using a ligature and the lungs were then fully inflated (pressure of 25

cm of water) by intratracheal instillation of glutaraldehyde (2.5% $wt.vol^{-1}$) for 30

minutes. The left main bronchus was then tied closed at the hilum so that the

volume of air spaces, airways and vessels was maintained constant, the left lung

then separated and immersed in fixative overnight.

Left lung volumes were measured by water displacement[18]. The left lung was

then processed for stereological quantification of the pulmonary vascular bed[18, 19]. In

brief, the lung was divided into multiple blocks from a random start point and blocks

selected for embedding in araldite resin using a systematic randomized strategy.

Tissue blocks were embedded in spherical moulds to ensure sectioning in

isotropically uniformly random orientations. Semithin sections (1µm) were cut from

each of the resin-embedded blocks and stained with toluidine blue.

Image analysis

Randomly acquired images (Olympus BX61 motorised microscope) of the tissue

sections were digitized (Olympus DP70 digital camera) and displayed on screen to

permit superimposition of stereologic grids for analysis using a computer-assisted

stereological toolbox (CAST) system (Visiopharm integrator system version 2.9.11.0;

Olympus). All slides were identified by code so that the observer was blinded to the

experimental conditions. Pulmonary vascular remodeling was assessed in the intra-

acinar vessels. A counting frame with two inclusion and two exclusion boundaries

(Supplemental Figure 1) was used to determine the length density of the vessels

within the gas exchange region of the lung (intra-acinar vessels) and unbiased

selection of vessels for direct measurement of lumen diameter. Using this strategy

the probability of selection of a vessel for lumen diameter measurement was directly

proportional to the total length of vessel within the lung in that diameter category[18].

The lumen diameter was taken as the maximum distance across the lumen

measured perpendicular to a line drawn along the longest axis of the image of the

transected lumen (Supplemental Figure 1). The external diameter of the vessels was

measured at the same position as the lumen diameter. Wall thickness was

calculated as half the difference between the external and internal (lumen) diameters.

A point counting grid was also included that allowed determination of the volume

fraction of the vascular lumen within the lung. Intra-acinar vessels were identified as

those accompanying respiratory bronchioles or more distal airways and alveoli which

had a lumen diameter greater than 10 microns and less than 50 microns.

Statistical Analyses

Normally distributed data are reported as means (±SEM) while non-normally

distributed data are presented as medians ± inter quartile range (IQR).   For normally

distributed data, determination of the statistical significance of differences between

two groups means in planned a priori comparisons were made using paired or

unpaired t-tests as appropriate. For non-normally distributed data statistical significance was determined using the Mann-Whitney U or Wilcoxon tests; p-values were computed using the exact (permutation) method. Multiple post hoc comparisons across experimental groups were made using the Holms-Sidak step-down test to correct for multiple comparisons[20]. Statistical analysis was undertaken using PASW 18 (formerly SPSS), IBM. Values of P<0.05 were accepted as statistically significant.

Supplemental Tables

Supplemental Table 1. Mean (±SEM) vessel length density in the lungs of the four experimental groups following three weeks of hypoxic exposure.

	Wild-type (grem1+/+)		Haplodeficient (grem1+/-)	
	Normoxia	Hypoxia	Normoxia	Hypoxia
Vessel length density (cm.cm^{-3})	2461 (±151)	2024* (±110)	2390 (± 135)	2132 (± 104)

There was a significant decrease in pulmonary intra-acinar vessel density in the wild-type mice following long-term hypoxic exposure that was not observed in the grem1$^{+/-}$ haplodeficient mice. n=8 per group. * signifies significant differences from matched normoxic control, *P*<0.05*.*

Supplemental Table 2. The total increase in pulmonary vascular resistance (PVR), the vasoconstricor (Y-27632 reversible) component, the difference between these two and the calculated component caused by vascular remodeling (determined using Poiseuille's equation) in chronically hypoxic wild-type and haplodeficient (grem1$^{+/-}$) mouse lungs.

	Total PVR increase	Constriction (Y-27632)	Difference	Remodelling (Poiseuille)
Wild-type (Grem1$^{+/+}$)	0.85* (0.032)	0.37* (0.04)	0.47* (0.04)	0.54* (0.089)
Grem1$^{+/-}$	0.63*# (0.043)	0.33* (0.03)	0.32*# (0.04)	0.27*# (0.14)

Values are means (±SEM). All values in chronically hypoxic mouse lungs are expressed normalised to the mean normoxic values. Total PVR increase was calculated as the measured increase in PVR in each chronically hypoxic lung divided by the mean normoxic PVR. The vasoconstrictor component was calculated as the reduction in PVR induced by Y27632 divided by the mean normoxic PVR. The difference between the total PVR and the Y27632-induced reduction was taken to approximate the component of the chronic hypoxia-induced increase that was caused by vascular remodelling. The predicted increase in PVR due to structural change was calculated based on the stereologically derived data on vascular structure. As the total length of vessels in the lung was unchanged following hypoxic exposure (Figure 7D), the structural component of the increase in PVR was caused solely by reduction in the radius of the lumen. Thus the change in the structural
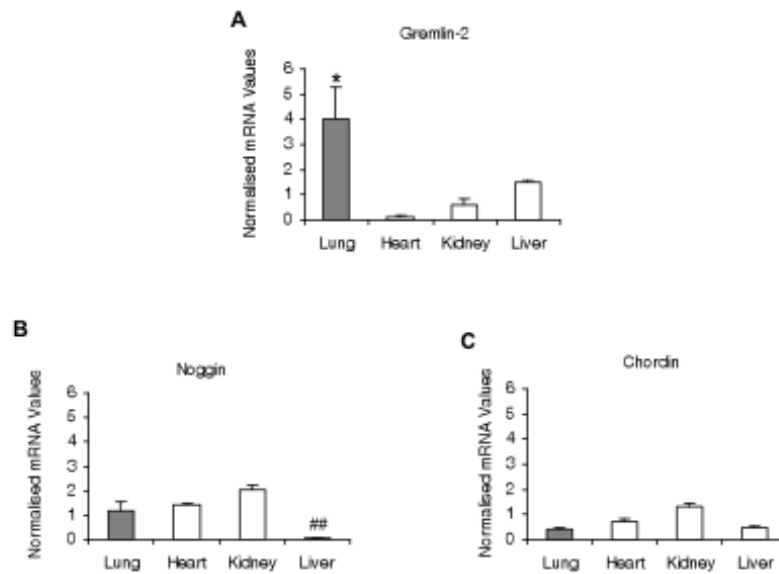
component of the increase in PVR was modelled using Poiseuilles equation in which

baseline vascular radius was taken to be the mean vessel radius in normoxic lungs.

In both wild-type and haplodeficient mouse lungs the hemodynamically determined

structural component of PVR (Difference) and the calculated structural component

based on the measured changes in vascular structure are similar in magnitude.

Furthermore, it can be seen that the reduction in chronic hypoxic PVR caused by

gremlin haplodefidiency was entirely due to a reduction in the structural component

of the hypoxia-induced increase. * indicates statistically significant difference from 0

i.e. normoxia (P<0.01). # indicates statistically significant difference from wild-type

value (P<0.05).
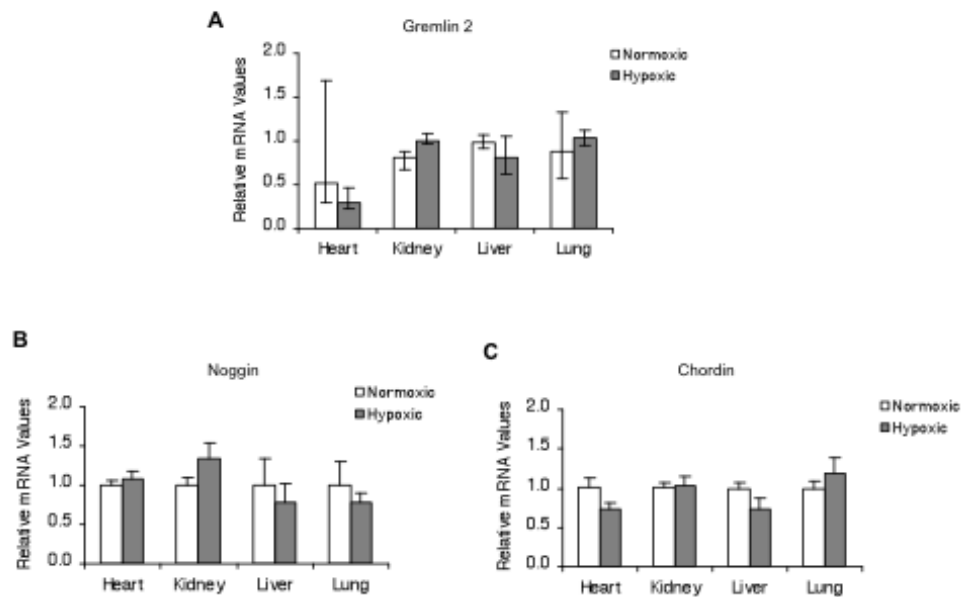
Supplemental Figures and Figure Legends.

Supplemental Figure 1. Image showing method of stereological analysis of vessel lumen diameter and wall thickness - inclusion/exclusion frame. A counting frame was superimposed over randomly acquired images of lung tissue sections using CAST software. When the lumen of an intra-acinar vessel fell on the green line (inclusion line) or inside the frame it was counted and the internal and external diameters measured at a site perpendicular to the longest axis (dotted line). If the lumen of a vessel fell on the red line (exclusion line) it was excluded. x20 objective, scale bar represents 100μm.
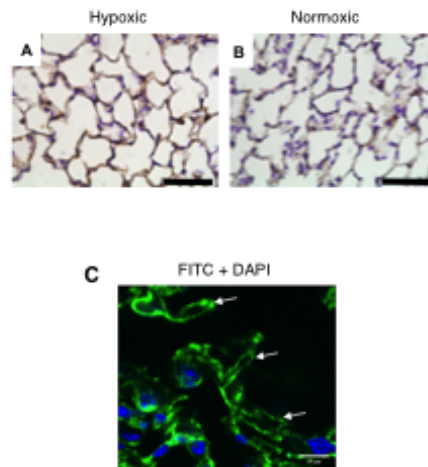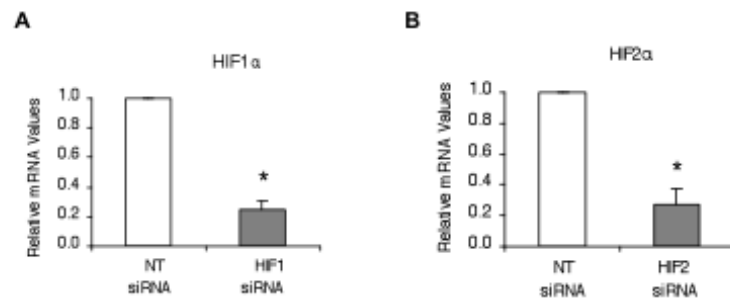
Supplemental Figure 2. High basal gremlin 2 (also known as protein related to dan and cerebrus, PRDC) expression in the lung. (**A**) The secreted BMP antagonist gremlin 2 (mean±SE), which is highly homologous to gremlin 1, was more highly expressed in the lung compared to the systemic organs. The other well characterized secreted BMP2 and BMP4 antagonists noggin (**B**) and chordin (**C**) did not show the disproportionately high expression levels shown by gremlin 1 and gremlin 2 (mean±SE) (n=7). Values are normalized to 18S RNA. * indicates significant difference from all other organs ($P<0.05$). ## indicates significant difference of liver from other organs ($P<0.01$).
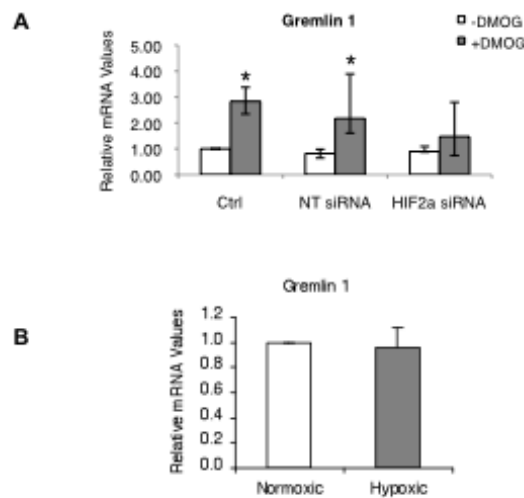
Supplemental Figure 3. The BMP antagonists gremlin 2, noggin and chordin were unaltered in response to hypoxia. (**A**) The secreted BMP antagonist gremlin 2 (median±IQR) which is highly homologous to gremlin 1 was not altered in response to two days of hypoxic exposure in any of the organs analyzed. Values are normalized to 18S RNA and expressed as fold-change relative to normoxic control for each organ. The other secreted BMP antagonists noggin (**B**) and chordin (**C**) also remained unchanged in response to hypoxia (mean±SE) (*n*=7). Values are normalized to 18S RNA and expressed as fold-change relative to normoxic control for each organ.
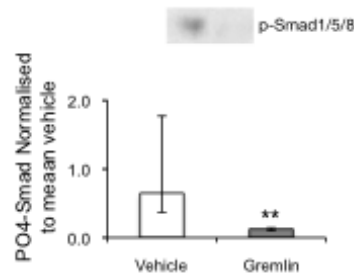
Supplemental Figure 4. Representative images showing gremlin within the alveolar wall. Immunohistochemical staining (brown) of gremlin in a mouse lung showed increased gremlin expression within the alveolar walls following 48 hours of hypoxic exposure (A) when compared to basal normoxic (B) conditions. (x40 objective). Scale bar represents 50μm. (C) Representative confocal image of immunofluorescent (FITC) staining of gremlin in sections from a normoxic mouse lung demonstrated that the labelling in the alveolar wall was observed in a pattern suggesting its localization predominantly in the capillary endothelium (x63 oil immersion objective). Scale bar represents 10 microns.
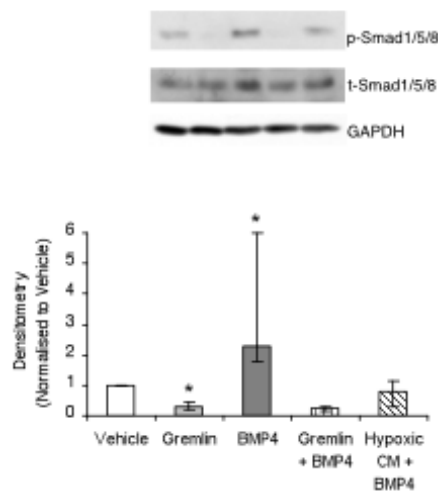
Supplemental Figure 5. Successful knockdown (mean±SE) of HIF1α and HIF2α by their respective targeting siRNA was confirmed by Real-Time PCR. Values (n=7 in each group) were normalised to 18S RNA and expressed as fold-change relative to the normoxic control mean (ctrl –siRNA).
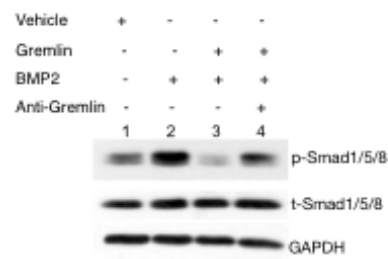
Supplemental Figure 6. **(A)** The prolyl hydroxylase inhibitor dimethyloxalylglycine (DMOG) induced increases in gremlin 1 expression in pulmonary endothelial cells that required HIF2a. Under control conditions in the absence of siRNA (Ctrl) and in the presence of non-targeting siRNA (NT siRNA), DMOG (10^{-3}M) caused significant increases in gremlin 1 expression (median±IQR). siRNA mediated knockdown of HIF2a blocked the DMOG induced response of gremlin (HIF2a siRNA). Note that in the absence of DMOG siRNA did not significantly alter gremlin expression (non-targeting and siRNA targeting HIF2a). Values are shown as medians ±inter quartile ranges (n=6-7 per group) * indicates significant difference from matched normoxic group ($P<0.05$, Wilcoxon signed rank). **(B)** Gremlin 1 expression in human pulmonary artery smooth muscle cells was not significantly altered by two days of hypoxic exposure. Gremlin 1 mRNA expression (mean±SE) in PASMCs in response to 48 hours hypoxic exposure (*n*=4). Values are normalised to 18S RNA and expressed as fold-change relative to normoxic control.

Supplemental Figure 7. Gremlin 1 inhibits basal Smad1/5/8 phosphorylation in human pulmonary microvascular endothelial cells. Treatment with recombinant gremlin 1 (2 micrograms/ml) for 1 hour significantly reduced basal Smad1/5/8 phosphorylation in these pulmonary endothelial cells. Densitometric analysis showed a statistically significant (**$P<0.01$) reduction in Smad1/5/8 phosphorylation following gremlin 1 treatment (median±IQR). Values were normalized to vehicle control value (n=6).
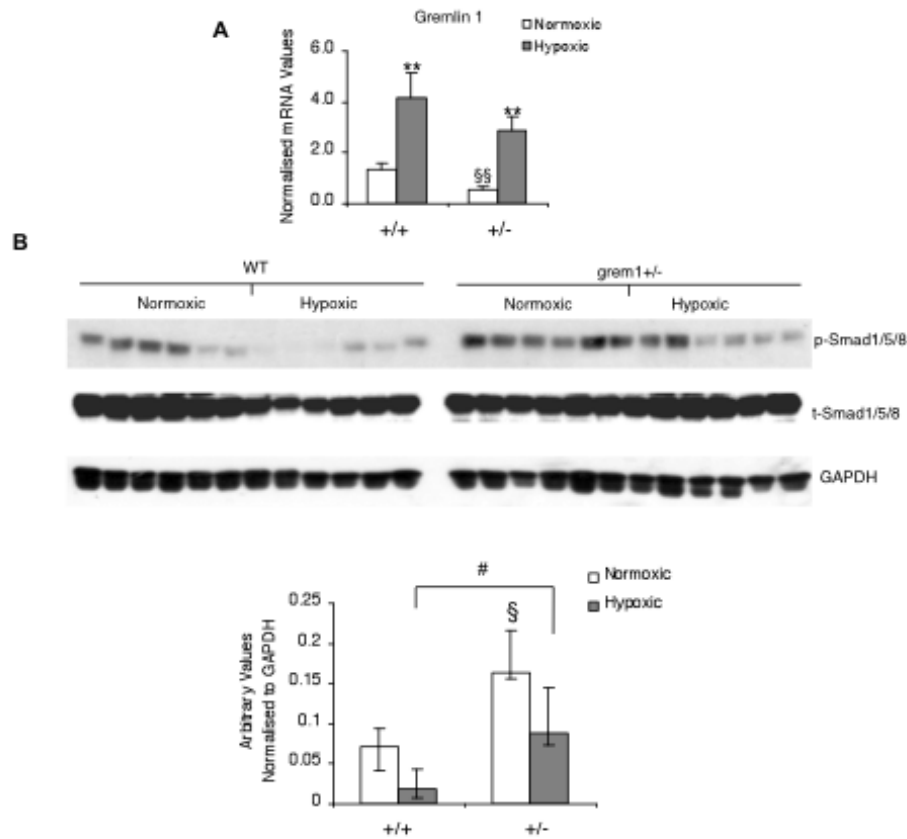
Supplemental Figure 8. BMP4 induces Smad1/5/8 in human pulmonary microvascular endothelial cells, which is similarly blocked by both recombinant gremlin 1 and hypoxia conditioned medium. Western blot showing Smad1/5/8 phosphorylation in pulmonary endothelial cells following treatment for one hour with vehicle, gremlin 1, recombinant BMP4, recombinant BMP4 together with recombinant gremlin 1, and BMP4 together with hypoxic conditioned medium respectively. Hypoxic conditioned medium was medium removed from pulmonary microvasclar endothelial cells that had been cultured in hypoxia for 48 hours. Densitometric analysis (median±IQR) showed that BMP4 treatment caused a significant increase in Smad1/5/8 phosphorylation whereas this action was not observed in the presence of gremlin 1 or hypoxia conditioned medium (n=6 per group). Gremlin 1 treatment alone reduced Smad1/5/8 phosphorylation significantly below that observed in the vehicle treated group. * and ** indicate significant difference from vehicle treatment (P<0.05 and <0.01 respectively).

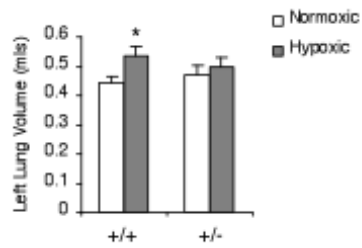|	1	2	3	4
Vehicle	+	-	-	-
Gremlin	-	-	+	+
BMP2	-	+	+	+
Anti-Gremlin	-	-	-	+

p-Smad1/5/8

t-Smad1/5/8

GAPDH

Supplemental Figure 9. Polyclonal goat anti-gremlin antibody blocks gremlin function. Western blot showing that BMP2 treatment for 1 hour induced Smad1/5/8 phosphorylation in human pulmonary microvascular endothelial cells (lane 2) that was blocked by recombinant gremlin 1 (lane 3). Anti-gremlin antibody prevented the inhibitory action of gremlin 1 on BMP2-induced Smad 1/5/8 phosphorylation (lane 4).

Supplemental Figure 10. Gremlin 1 expression and BMP signaling in grem1^{+/-} and wild-type mice lungs. (**A**) Basal gremlin 1 mRNA expression (mean±SE) in grem1^{+/-} is significantly less than that in wild-type mice lungs and is upregulated in response to 2 days of hypoxic exposure in both groups (n=8). (**B**) Smad1/5/8 phosphorylation (median±IQR) is higher in normoxic grem1^{+/-} mice lungs than in normoxic wild-type mice lungs. Similarly Smad1/5/8 phosphorylation is higher in hypoxic grem1^{+/-} mice lungs than in normoxic wild-type mice lungs (n=6). [§] indicates significant difference between normoxic wild-type and normoxic grem1^{+/-} mice (P<0.05). [#] indicates significant difference between hypoxic wild-type and hypoxic grem1^{+/-} mice (P<0.05).

Supplemental Figure 11. The mean left lung volume (mean±SE) of the wild-type hypoxic mice was significantly larger than that of normoxic wild type mice. No significant difference was observed between the two grem1^{+/-} groups. Thus, grem1^{+/-} mice did not show the increased lung volume normally observed in response to chronic hypoxia [15, 21-23].

Supplemental References

1. Roxburgh SA, Kattla JJ, Curran SP, O'Meara YM, Pollock CA, Goldschmeding R, Godson C, Martin F, Brazil DP. Allelic Depletion of grem1 Attenuates Diabetic Kidney Disease. *Diabetes.* 2009;58(7):1641-1650.

2. Khokha MK, Hsu DR, Brunet LJ, Dionne MS, Harland RM. Gremlin is the BMP antagonist required for maintenance of Shh and Fgf signals during limb patterning. *Nat Genet.* 2003;34:303 - 307.

3. Costello CM, Howell K, Cahill E, McBryan J, Konigshoff M, Eickelberg O, Gaine S, Martin F, McLoughlin P. Lung-selective gene responses to alveolar hypoxia: potential role for the bone morphogenetic antagonist gremlin in pulmonary hypertension. *Am J Physiol Lung Cell Mol Physiol.* 2008;295(2):L272-284.

4. Kiyono M, Shibuya M. Inhibitory Smad transcription factors protect arterial endothelial cells from apoptosis induced by BMP4. *Oncogene.* 2006;25(54):7131-7137.

5. Star GP, Giovinazzo M, Langleben D. Effects of bone morphogenic proteins and transforming growth factor-beta on In-vitro production of endothelin-1 by human pulmonary microvascular endothelial cells. *Vascular Pharmacology.* 2009;50(1-2):45-50.

6. Zhang S, Fantozzi I, Tigno DD, Yi ES, Platoshyn O, Thistlethwaite PA, Kriett JM, Yung G, Rubin LJ, Yuan JXJ. Bone morphogenetic proteins induce apoptosis in human pulmonary vascular smooth muscle cells. *Am J Physiol Lung Cell Mol Physiol.* 2003;285(3):L740-754.

7. Rothhammer T, Bataille F, Spruss T, Eissner G, Bosserhoff AK. Functional implication of BMP4 expression on angiogenesis in malignant melanoma. *Oncogene.* 2006;26(28):4158-4170.

8. Maciel TT, Melo RS, Schor N, Campos AH. Gremlin promotes vascular smooth muscle cell proliferation and migration. *Journal of Molecular and Cellular Cardiology.* 2008;44(2):370-379.

9. Morrell NW, Yang X, Upton PD, Jourdan KB, Morgan N, Sheares KK, Trembath RC. Altered Growth Responses of Pulmonary Artery Smooth Muscle Cells From Patients With Primary Pulmonary Hypertension to Transforming Growth Factor-{beta}1 and Bone Morphogenetic Proteins. *Circulation.* 2001;104(7):790-795.

10. Suzuki Y, Montagne K, Nishihara A, Watabe T, Miyazono K. BMPs Promote Proliferation and Migration of Endothelial Cells via Stimulation of VEGF-A/VEGFR2 and Angiopoietin-1/Tie2 Signalling. *J Biochem.* 2008;143(2):199-206.

11. Mitola S, Ravelli C, Moroni E, Salvi V, Leali D, Ballmer-Hofer K, Zammataro L, Presta M. Gremlin is a novel agonist of the major proangiogenic receptor VEGFR2. *Blood.* 2011;116(18):3677-3680.

12. Wordinger RJ, Fleenor DL, Hellberg PE, Pang IH, Tovar TO, Zode GS, Fuller JA, Clark AF. Effects of TGF-beta2, BMP-4, and gremlin in the trabecular meshwork: implications for glaucoma. *Invest Ophthalmol Vis Sci.* 2007;48(3):1191-1200.

13. Weissmann N, Akkayagil E, Quanz K, Schermuly RT, Ghofrani HA, Fink L, Hanze J, Rose F, Seeger W, Grimminger F. Basic features of hypoxic

pulmonary vasoconstriction in mice. *Respir Physiol Neurobiol.* 2004;139(2):191-202.

14.   Cadogan E, Hopkins N, Giles S, Bannigan JG, Moynihan J, McLoughlin P. Enhanced expression of inducible nitric oxide synthase without vasodilator effect in chronically infected lungs. *Am J Physiol Lung Cell Mol Physiol.* 1999;277(3):L616-627.

15.   Hyvelin J-M, Howell K, Nichol A, Costello CM, Preston RJ, McLoughlin P. Inhibition of Rho-Kinase Attenuates Hypoxia-Induced Angiogenesis in the Pulmonary Circulation. *Circ Res.* 2005;97(2):185-191.

16.   von Bethmann AN, Brasch F, Nusing R, Vogt K, Volk HD, Muller KM, Wendel A, Uhlig S. Hyperventilation induces release of cytokines from perfused mouse lung. *American journal of respiratory and critical care medicine.* 1998;157(1):263-272.

17.   Perk K, Frei YF, Herz A. Osmotic Fragility of Red Blood Cells of Young and Mature Domestic and Laboratory Animals. *Am J Vet Res.* 1964;25:1241-1248.

18.   Howell K, Costello CM, Sands M, Dooley I, McLoughlin P. L-Arginine promotes angiogenesis in the chronically hypoxic lung: a novel mechanism ameliorating pulmonary hypertension. *Am J Physiol Lung Cell Mol Physiol.* 2009;296(6):L1042-1050.

19.   Howell K, Preston RJ, McLoughlin P. Chronic hypoxia causes angiogenesis in addition to remodelling in the adult rat pulmonary circulation. *The Journal of Physiology.* 2003;547(1):133-145.

20.   Ludbrook J. Multiple comparison procedures updated. *Clinical and experimental pharmacology & physiology.* 1998;25(12):1032-1037.

21.   Cunningham EL, Brody JS, Jain BP. Lung growth induced by hypoxia. *J Appl Physiol.* 1974;37(3):362-366.

22.   Howell K, Preston RJ, McLoughlin P. Chronic hypoxia causes angiogenesis in addition to remodelling in the adult rat pulmonary circulation. *J Physiol.* 2003;547(Pt 1):133-145.

23.   Rabinovitch M, Gamble W, Nadas AS, Miettinen OS, Reid L. Rat pulmonary circulation after chronic hypoxia: hemodynamic and structural features. *Am J Physiol.* 1979;236(6):H818-827.

SUPPLEMENTAL MATERIAL

Gremlin plays a key role in the pathogenesis of pulmonary hypertension.

Edwina Cahill PhD[1], Christine M. Costello PhD[1], Simon C Rowan BSc[1], Susan Harkin[1], Katherine Howell PhD[1], Martin O. Leonard PhD[1], Mark Southwood PhD[3], Eoin P Cummins PhD[1], Susan F Fitzpatrick BSc[1], Cormac Taylor PhD[1], Nicholas W. Morrell MD[3], Finian Martin PhD[2], Paul McLoughlin MB BCh PhD[1,#]

[1]University College Dublin, School of Medicine and Medical Sciences and [2]School of Biomedical and Biomolecular Sciences, Dublin, Ireland and [3]University of Cambridge School of Clinical Medicine, Cambridge, United Kingdom.

[#]Correspondence should be addressed to:

Dr Paul McLoughlin MB BCh PhD.

University College Dublin,

School of Medicine and Medical Sciences,

Belfield, Dublin 4, Ireland.

e-mail.   Paul.mcloughlin@ucd.ie

Phone.   +353 1 716 6583.   Fax.   +353 1 716 6649

Supplemental Methods

Mice. All procedures involving mice were approved by the UCD Animal Research Ethics Sub-Committee and carried out under license from the Department of Health.

Chronic hypoxic pulmonary hypertension was induced by housing male C57BL/6 mice (10-12 weeks) in a hypoxic normobaric opaque perspex environmental chamber ($FiO_2 < 0.10$, $FiCO_2 < 0.01$) and weight-matched normoxic mice were maintained in normoxic conditions in the same room ($FiO_2 = 0.21$, $FiCO_2 < 0.01$). Oxygen concentrations were monitored using an automated gas analyzer (Pro-Ox and Pro-CO_2, Biospherix). The chamber was opened every 1-2 days for approximately 30 minutes to allow for changing of cages and replacement of food and water. Excess CO_2 produced by the mice was removed using a tray of soda lime placed inside the chamber. All mice were maintained in a specific pathogen-free (SPF) facility with free access to water and food.

Gremlin1 heterozygote knockout mice (grem1^{+/-}) were bred and pups genotyped by extracting DNA from ear punches and determining the presence of the LacZ knock-in gene by end-point PCR as described previously[1, 2].

RNA Isolation and real-time PCR. Total RNA was extracted from snap-frozen whole tissue or cells using a Qiagen RNeasy kit (RNeasy Mini Kit, Qiagen) and reverse-transcribed (RT) to cDNA using Superscript II RNase H-Reverse Transcriptase kit (Invitrogen) as previously described[3]. TaqMan real-time PCR was performed using 18S rRNA as the endogenous loading control gene. Reactions were carried out on the ABI PRISM 7900 Sequence Detection System with TaqMan Universal PCR Master Mix and TaqMan Gene Expression Assays (Applied Biosystems). Relative quantification of mRNA expression levels was determined using the standard curve method and normalised to 18S.

Immunohistochemical analysis

To obtain mouse lung sections, male C57BL/6 mice (*n*=5) were maintained in normoxia or exposed to 10% oxygen for two days. The mice were killed by exsanguination under general anesthesia, the lungs removed and then fixed by intratracheal instillation of paraformaldehyde (4%) at standard pressure (25 cm of water). The lungs were then immersed in paraformaldehyde and left overnight, cut into blocks, embedded in paraffin wax and sections (7µm) cut and mounted onto poly-l-lysine-coated glass slides (Sigma-Aldrich). Immunohistochemistry was performed as previously described using goat anti-gremlin antibody (R&D Systems)[3]. No staining was detected when gremlin primary antibody was omitted or substituted with an irrelevant antibody also raised in goat (anti-HAND1, R&D Systems).

Specimens from human lungs with IPAH (*n* = 2) and FPAH (*n* = 2) were obtained at time of transplant while control specimens were obtained from lung tissue resected during surgery for cancer at a site remote from the tumor margins. All patients had provided full written consent. Sections were prepared and immunostained for gremlin as above.

Immunoflourescence Staining

Mouse lungs were fully inflated using paraformaldehyde (1%) for 30mins and then placed into sucrose solutions (30%) at 4˚C for 24 hours before infiltration with OCT compound (Tissue Tek®, Sakura Finetek). Sections (10 microns) were cut and mounted onto poly-L-lysine coated slides for immunostaining and fluorescent labelling using the tyramide signal amplification (TSA™ Biotin System, Perkin Elmer Inc.). Slides were immersed in glycine (100mM) for 45 minutes to quench formaldehyde-induced fluorescence followed by immersion in sodium borohydride

3

(0.1%) for 30mins. Slides were washed and blocked in TNB blocking buffer (supplied in TSA™ kit) for 30mins, and incubated with anti-gremlin antibody (R&D Systems) overnight at 4°C. Slides were then incubated in biotinylated rabbit anti-goat secondary antibody (Vector Laboratories) for 1 hour, washed, and incubated in streptavidin-HRP (supplied in TSA™ kit) and subsequently biotinyl tyramide amplification reagent (supplied in TSA™ kit). FITC-streptavidin (Sigma-Aldrich) was added for 1 hour. Tissue sections were counterstained with 4',6-diamidino-2-phenylindole (Sigma-Aldrich) and mounted using Vectashield (Vector Laboratories). Images were acquired using a confocal laser-scanning microscope (Zeiss, LSM 510 Meta, x40/NA1.3 and x63/NA1.4 oil immersion objectives). No fluorescence was observed when gremlin primary antibody was omitted.

Western Blotting and ELISA

Western blot analysis was performed using whole lung and cell lysates that were lysed in radioimmuno-precipitation assay (RIPA) buffer supplemented with serine protease inhibitor, phenlyethanesulfonylflouride (PMSF), and a cocktail of protease and phosphatase inhibitors (Sigma-Aldrich). Tissue was homogenised (Ultra-Turrax T8, Carl Stuart) and cells were lysed by repetitive vortexing. Total protein content was determined using the bicinchoninic acid (BCA) assay (Pierce). Cell conditioned medium was concentrated using 5kDa Ultra-15 filters (Millipore) by centrifugation in a swinging bucket rotor (4000g for 45mins at 4°C). Protein extracts were separated by 15% (vol/vol) SDS-PAGE and blotted using: rabbit p-Smad1/5/8 (Cell Signaling Technology), rabbit total Smad1/5/8 (Santa Cruz Biotechnology), goat gremlin (R&D Systems), goat BMPR2 (R&D Systems), rabbit BMP2 and BMP4 (Abcam). These were detected with the respective, species-specific horseradish peroxidise-

conjugated secondary antibodies (Dako and Chemicon). Densitometry was performed using ImageJ software normalising to GAPDH or vehicle.

An Enzyme-Linked Immunosorbent Assay (ELISA) (R&D Systems) was used to examine the presence of secreted BMP ligands in concentrated conditioned medium from HMVEC-L. ELISAs were performed according to the protocols provided by the manufacturer (R&D Systems).

Cell Culture

For *in vitro* studies, primary human pulmonary microvascular endothelial cells from lung (HMVEC-L) and primary smooth muscle cells isolated from human pulmonary artery (PASMC) were bought in from Lonza Bioscience (formerly Cambrex). Cells were grown on sterile tissue culture dishes in Endothelial Growth Medium (EGM-2MV; Code: CC-3202) or Smooth Muscle Growth Medium (SmGM-2; Code CC-3182) according to the manufacturers instructions. All cells used in these experiments were passage 6-7 and were routinely checked for mycoplasma contamination using the VenorGeM PCR kit (Cambio Ltd). For hypoxic experiments, cells were placed in a hypoxic chamber (Coy Labs) and cultured in an atmosphere of 1% O_2, 5% CO_2 and 94% N_2 for 48 hours. Control conditions were achieved by culture in 21% O_2, 5% CO_2 and 74% N_2 in a cell-culture incubator.

To knock-down endogenous HIF1α or HIF2α, cells (HMVEC-L) were transfected with 10nM of a Smartpool HIF1α or HIF2α-specific siRNA respectively (Dharmacon) using lipofectin (Invitrogen Life Technologies). A non-targeting Smartpool siRNA was used as a negative control. Cells were grown on 6 well plates in EGM-2MV medium without antibiotics. When cells were 30-40% confluent, cells were transfected using Optimem reduced-serum media for 4 hours. Following

transfection cells were placed in normoxic or hypoxic (1% O_2) conditions for a further 48 hours. HIF1α and HIF2α mRNA expression levels were measured by Real-Time RT-PCR to confirm effective reduction with specific siRNA. Gremlin 1 expression was also analysed by Real-Time RT-PCR.

For Smad1/5/8 phosphorylation experiments hypoxic serum-free conditioned medium (CM) was taken off cells that were incubated in hypoxia for 48 hours and briefly centrifuged to remove dead cells. For detection of Smad1/5/8 phosphorylation, cells were serum-starved overnight in serum-free medium (SFM) containing supplements and treatments were added the following day for 1 hour as follows: 2 microngrams/ml of recombinant gremlin 1, 80ng/ml of BMP4 or 100ng/ml of BMP2 (all from R&D Systems). To block gremlin 1 antagonizing activity, 15 micrograms/ml of anti-gremlin antibody (R&D Systems) was pre-incubated with hypoxic conditioned medium or recombinant gremlin 1 for 1 hour prior to treatment. In all experiments in which hypoxia conditioned medium was not added unconditioned medium was added instead.

The concentrations of recombinant BMP2 (100ng/ml) and BMP4 (80mn/ml) used were chosen from within the range of concentrations previously reported[4-10]. In pilot experiments, we confirmed that the chosen concentrations accelerated wound healing compared to vehicle but did not cause complete wound closure; thus the effect of any further intervention, which *a priori* might either have reduced or augmented the effect of the BMPs, could be detected.

The concentration of recombinant gremlin used (2mg/ml) was selected based on previously published reports[11,12]. In pilot experiments we confirmed that this concentration blocked BMP2-induced Smad phosphorylation. We then confirmed that we had identified a concentration of gremlin that produced an inhibitory effect on

BMP2-induced Smad phosphorylation and endothelial wound healing similar to that of hypoxia conditioned medium. These findings suggest that the concentration of recombinant gremlin we used produced local concentrations of biologically active gremlin in the endothelial cell microenvironment similar to those produced by hypoxic endothelial cells.

For scratch healing assays HMVEC-L were seeded and allowed to grow to a confluent monolayer and a single vertical scratch was applied to each chamber using a 10-100 microlitre pipette tip (Greiner). Treatments were added in low-serum medium (3%) for 24 hours and percentage wound closure was measured using ImageJ software as previously described[3]. Hypoxia conditioned medium for these experiments was prepared as described above. In all experiments in which hypoxic conditioned medium was not added, unconditioned medium was added instead. Six fields of view in each well were measured at the pre-defined positions (above and below each drawn line) and each experiment was repeated six times.

Assessment of hypoxia-induced changes in pulmonary vascular resistance

Pulmonary hemodynamic responses were assessed using an isolated ventilated lung preparation perfused at constant flow, as previously described[13]. This preparation permits direct assessment of pulmonary vascular resistance independently of alterations in cardiovascular function, reflex, hormonal or other factors changed by chronic hypoxia[14-16]. Wild-type and grem1^{+/-} mice were exposed to hypoxic (F_IO_2=0.10) conditions in a normobarbic environmental chamber or maintained in normoxia (F_IO_2=0.21) in the same room for 3 weeks, as previously described[15]. The hypoxic chamber was opened for 30 minutes every 1-2 days for

changes of water, feed and bedding and removal of mice from, or additon of mice to, the chamber.

Following exposure, mice were then anaesthetised (70mg.kg^{-1} sodium pentobarbitone (Rhône Merieux Ltd, Harlow, UK) intraperitoneally and anti-coagulated (1000 units kg^{-1} heparin). A cannula was then inserted into the trachea via tracheostomy and the mouse ventilated (5% CO_2 in air, tidal volume of 250µl, respiratory frequency 90). The femoral artery was then exposed and the mouse killed by exsanguination. A sample of blood was obtained for measurement of hematocrit. A midline incision was made through the sternum and the ribs retracted to expose the heart and lungs. A cannula was then inserted into the pulmonary artery and left atrium. The lungs were perfused (2ml/min) with DMEM heated to 37°C, pH 7.45 with Ficoll (4 g/100ml, PM 70, Sigma-Aldrich) according to standard protocols[13] and were hyperinflated to an airway pressure of 15cmH$_2$O every 5 minutes. End expiratory pressure was set to 1.6 mmHg and the venous outflow pressure to 2 mmHg. Following stabilization of the preparation, pressure measurements were recorded as the mean of 10 determinations made at end expiration during consecutive breaths, thus ensuring that vascular pressures and resistance were determined in Zone 3 conditions. Measurements were made in the final minute prior to a regular hyperinflation. In a subset of lungs, the rho kinase inhibitor Y27632 (Merck Biosciences) was then added to the perfusate (10^{-5}M) and vascular pressures recorded once the reductions had stabilized[15].

After completion of the perfusion protocol, the hearts were separated from the lungs, fixed by immersion in paraformaldehyde (4%) and stored. The atria were removed at the level of the atrioventricular junction in the plane of the mitral and tricuspid annuli i.e. at the level of the openings of the tricuspid and mitral valves

where the valve leaflets attach. The ventricles were then transected parallel to this plane at two levels, one third and two thirds of the distance from the atrioventricular junction to the apex of the heart. The relative cross sectional areas of the cut surfaces of the right and left ventricles were determined at each of these two levels and the mean of the two results was taken as the value for that heart (RV:LV+S). The cross sectional areas of the cut surfaces of the right and left ventricle were determined by stereological analysis. Images of the cut curfaces were acquired, digitised and viewed under a superimposed stereological grid showing regularly spaced points (Visiopharm integrator system version 2.9.11.0; Olympus Denmark). Points landing on right ventricle and on left ventricle+septum were separately counted and the ratio of these two determined at each level. The mean of these two values was taken as the RV:LV+S for that heart.

Stereological Quantification of Pulmonary Vascular structure

Hypoxia induced changes in pulmonary vascular structure were assessed in separate groups of wild-type and grem1$^{+/-}$ mice exposed to hypoxic or normoxic conditions for 3 weeks. Mice were then anaesthetized (sodium pentobarbitone 70mg.kg^{-1}, Rhône Merieux Ltd) intraperitoneally and anti-coagulated (1000 units kg^{-1} heparin). A midline incision was made through the sternum and the ribs retracted to expose the lungs. Tracheal and pulmonary arterial cannulae were inserted into the pulmonary artery as described above. An incision was made in the apex of the left ventricle to facilitate free drainage of perfusate. Initially rho-kinase inhibitor (Y-27632 10^{-5}M, Merck Biosciences) in normal saline was perfused through the pulmonary circulation to inhibit ROCK activity and ensure complete relaxation of vasomotor tone[15]. Defibrinated horse blood (Cruinn Diagnostics Ltd.) was then perfused

9

through the vasculature (pulmonary arterial pressure 30cmH$_2$O above the hilum)

until the pulmonary vessels were uniformly filled. The presence of erthyrocytes in

the vascular space facilitated identification of vessels within the pulmonary

parenchyma following the preparation of sections for microscopic examination.

Horse erythrocytes are of similar size (average diameter 5.8 microns) to mouse red

blood cells (average diameter 6.1 microns)[17].   Once all the blood vessels had been

filled, as indicated by a uniformly red appearance of all lung lobes, the wound at the

apex of the left ventricle was closed using a vascular clamp ensuring that pressure

throughout the vessels was uniform (30cmH$_2$O). The pulmonary arterial trunk was

then tied closed using a ligature and the lungs were then fully inflated (pressure of 25

cm of water) by intratracheal instillation of glutaraldehyde (2.5% wt.vol^{-1}) for 30

minutes. The left main bronchus was then tied closed at the hilum so that the

volume of air spaces, airways and vessels was maintained constant, the left lung

then separated and immersed in fixative overnight.

Left lung volumes were measured by water displacement[18]. The left lung was

then processed for stereological quantification of the pulmonary vascular bed[18, 19]. In

brief, the lung was divided into multiple blocks from a random start point and blocks

selected for embedding in araldite resin using a systematic randomized strategy.

Tissue blocks were embedded in spherical moulds to ensure sectioning in

isotropically uniformly random orientations. Semithin sections (1µm) were cut from

each of the resin-embedded blocks and stained with toluidine blue.

Image analysis

Randomly acquired images (Olympus BX61 motorised microscope) of the tissue

sections were digitized (Olympus DP70 digital camera) and displayed on screen to

permit superimposition of stereologic grids for analysis using a computer-assisted

stereological toolbox (CAST) system (Visiopharm integrator system version 2.9.11.0;

Olympus). All slides were identified by code so that the observer was blinded to the

experimental conditions. Pulmonary vascular remodeling was assessed in the intra-

acinar vessels. A counting frame with two inclusion and two exclusion boundaries

(Supplemental Figure 1) was used to determine the length density of the vessels

within the gas exchange region of the lung (intra-acinar vessels) and unbiased

selection of vessels for direct measurement of lumen diameter. Using this strategy

the probability of selection of a vessel for lumen diameter measurement was directly

proportional to the total length of vessel within the lung in that diameter category[18].

The lumen diameter was taken as the maximum distance across the lumen

measured perpendicular to a line drawn along the longest axis of the image of the

transected lumen (Supplemental Figure 1). The external diameter of the vessels was

measured at the same position as the lumen diameter. Wall thickness was

calculated as half the difference between the external and internal (lumen) diameters.

A point counting grid was also included that allowed determination of the volume

fraction of the vascular lumen within the lung. Intra-acinar vessels were identified as

those accompanying respiratory bronchioles or more distal airways and alveoli which

had a lumen diameter greater than 10 microns and less than 50 microns.

Statistical Analyses

Normally distributed data are reported as means (±SEM) while non-normally

distributed data are presented as medians ± inter quartile range (IQR). For normally

distributed data, determination of the statistical significance of differences between

two groups means in planned a priori comparisons were made using paired or

unpaired t-tests as appropriate. For non-normally distributed data statistical

significance was determined using the Mann-Whitney U or Wilcoxon tests; p-values

were computed using the exact (permutation) method. Multiple post hoc

comparisons across experimental groups were made using the Holms-Sidak step-

down test to correct for multiple comparisons[20]. Statistical analysis was undertaken

using PASW 18 (formerly SPSS), IBM. Values of P<0.05 were accepted as

statistically significant.

Supplemental Tables

Supplemental Table 1. Mean (±SEM) vessel length density in the lungs of the four experimental groups following three weeks of hypoxic exposure.

	Wild-type (grem1+/+)		Haplodeficient (grem1+/-)	
	Normoxia	Hypoxia	Normoxia	Hypoxia
Vessel length density	2461	2024*	2390	2132
(cm.cm^{-3})	(±151)	(±110)	(± 135)	(± 104)

There was a significant decrease in pulmonary intra-acinar vessel density in the wild-type mice following long-term hypoxic exposure that was not observed in the grem1$^{+/-}$ haplodeficient mice. n=8 per group. * signifies significant differences from matched normoxic control, $P<0.05$.

Supplemental Table 2. The total increase in pulmonary vascular resistance (PVR), the vasoconstricor (Y-27632 reversible) component, the difference between these two and the calculated component caused by vascular remodeling (determined using Poiseuille's equation) in chronically hypoxic wild-type and haplodeficient (grem1$^{+/-}$) mouse lungs.

	Total PVR increase	Constriction (Y-27632)	Difference	Remodelling (Poiseuille)
Wild-type (Grem1$^{+/+}$)	0.85* (0.032)	0.37* (0.04)	0.47* (0.04)	0.54* (0.089)
Grem1$^{+/-}$	0.63*# (0.043)	0.33* (0.03)	0.32*# (0.04)	0.27*# (0.14)

Values are means (±SEM). All values in chronically hypoxic mouse lungs are expressed normalised to the mean normoxic values. Total PVR increase was calculated as the measured increase in PVR in each chronically hypoxic lung divided by the mean normoxic PVR. The vasoconstrictor component was calculated as the reduction in PVR induced by Y27632 divided by the mean normoxic PVR. The difference between the total PVR and the Y27632-induced reduction was taken to approximate the component of the chronic hypoxia-induced increase that was caused by vascular remodelling. The predicted increase in PVR due to structural change was calculated based on the stereologically derived data on vascular structure. As the total length of vessels in the lung was unchanged following hypoxic exposure (Figure 7D), the structural component of the increase in PVR was caused solely by reduction in the radius of the lumen. Thus the change in the structural

component of the increase in PVR was modelled using Poiseuilles equation in which baseline vascular radius was taken to be the mean vessel radius in normoxic lungs. In both wild-type and haplodeficient mouse lungs the hemodynamically determined structural component of PVR (Difference) and the calculated structural component based on the measured changes in vascular structure are similar in magnitude. Furthermore, it can be seen that the reduction in chronic hypoxic PVR caused by gremlin haplodefidiency was entirely due to a reduction in the structural component of the hypoxia-induced increase. * indicates statistically significant difference from 0 i.e. normoxia ($P<0.01$). [#] indicates statistically significant difference from wild-type value ($P<0.05$).
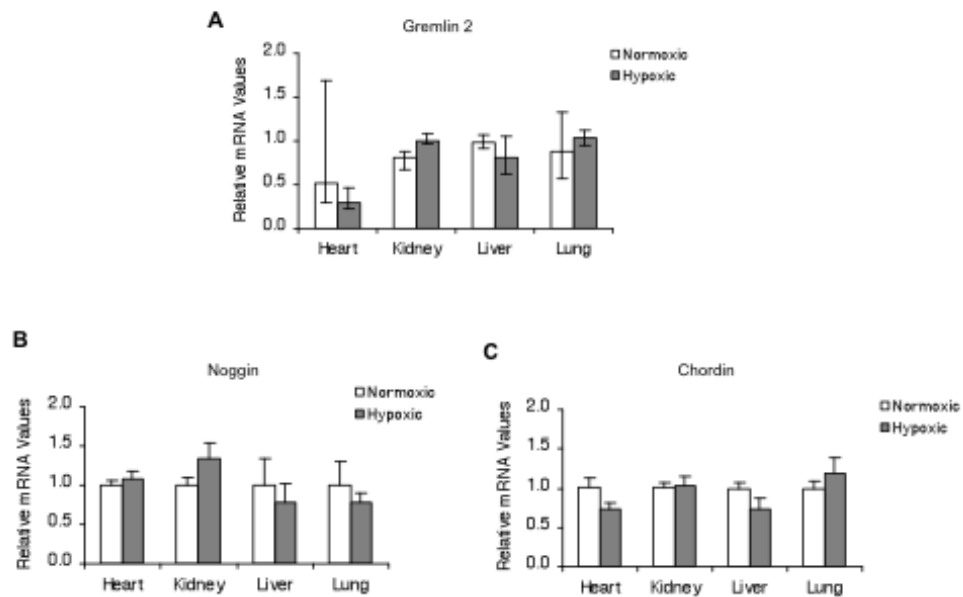
Supplemental Figures and Figure Legends.

Supplemental Figure 1. Image showing method of stereological analysis of vessel lumen diameter and wall thickness - inclusion/exclusion frame. A counting frame was superimposed over randomly acquired images of lung tissue sections using CAST software. When the lumen of an intra-acinar vessel fell on the green line (inclusion line) or inside the frame it was counted and the internal and external diameters measured at a site perpendicular to the longest axis (dotted line). If the lumen of a vessel fell on the red line (exclusion line) it was excluded. x20 objective, scale bar represents 100µm.
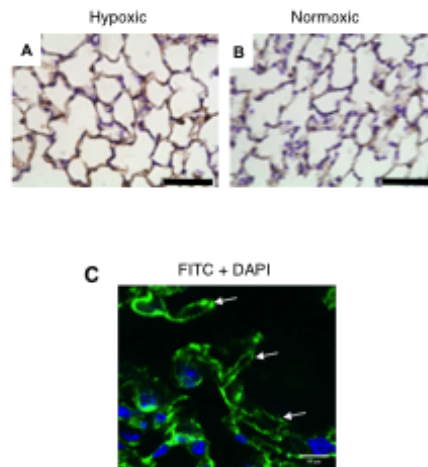
Supplemental Figure 2. High basal gremlin 2 (also known as protein related to dan and cerebrus, PRDC) expression in the lung. (**A**) The secreted BMP antagonist gremlin 2 (mean±SE), which is highly homologous to gremlin 1, was more highly expressed in the lung compared to the systemic organs. The other well characterized secreted BMP2 and BMP4 antagonists noggin (**B**) and chordin (**C**) did not show the disproportionately high expression levels shown by gremlin 1 and gremlin 2 (mean±SE) (n=7). Values are normalized to 18S RNA. * indicates significant difference from all other organs ($P<0.05$). ## indicates significant difference of liver from other organs ($P<0.01$).
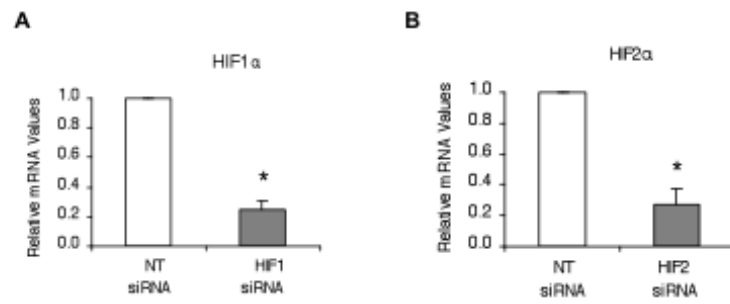
Supplemental Figure 3. The BMP antagonists gremlin 2, noggin and chordin were unaltered in response to hypoxia. (**A**) The secreted BMP antagonist gremlin 2 (median±IQR) which is highly homologous to gremlin 1 was not altered in response to two days of hypoxic exposure in any of the organs analyzed. Values are normalized to 18S RNA and expressed as fold-change relative to normoxic control for each organ. The other secreted BMP antagonists noggin (**B**) and chordin (**C**) also remained unchanged in response to hypoxia (mean±SE) (*n*=7). Values are normalized to 18S RNA and expressed as fold-change relative to normoxic control for each organ.
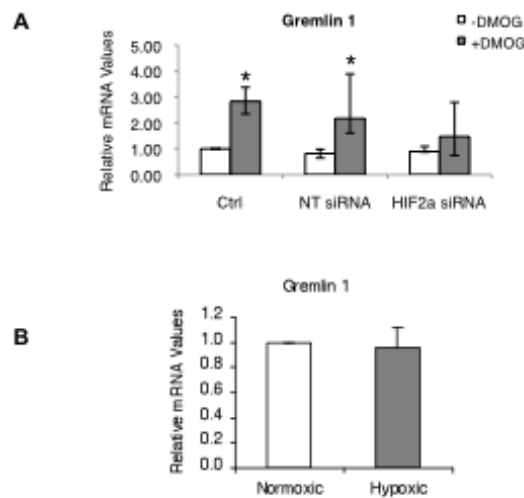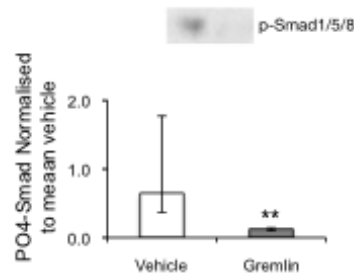
Supplemental Figure 4. Representative images showing gremlin within the alveolar wall. Immunohistochemical staining (brown) of gremlin in a mouse lung showed increased gremlin expression within the alveolar walls following 48 hours of hypoxic exposure (A) when compared to basal normoxic (B) conditions. (x40 objective). Scale bar represents 50µm. (C) Representative confocal image of immunofluorescent (FITC) staining of gremlin in sections from a normoxic mouse lung demonstrated that the labelling in the alveolar wall was observed in a pattern suggesting its localization predominantly in the capillary endothelium (x63 oil immersion objective). Scale bar represents 10 microns.
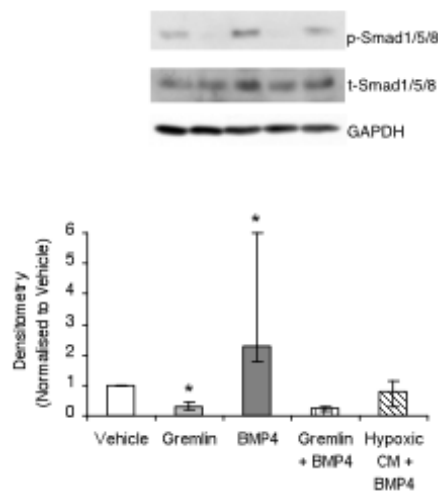
Supplemental Figure 5. Successful knockdown (mean±SE) of HIF1α and HIF2α by their respective targeting siRNA was confirmed by Real-Time PCR. Values (n=7 in each group) were normalised to 18S RNA and expressed as fold-change relative to the normoxic control mean (ctrl –siRNA).
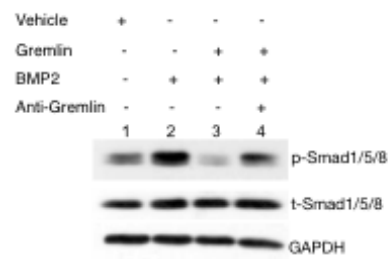
Supplemental Figure 6. **(A)** The prolyl hydroxylase inhibitor dimethyloxalylglycine (DMOG) induced increases in gremlin 1 expression in pulmonary endothelial cells that required HIF2a. Under control conditions in the absence of siRNA (Ctrl) and in the presence of non-targeting siRNA (NT siRNA), DMOG (10^{-3}M) caused significant increases in gremlin 1 expression (median±IQR). siRNA mediated knockdown of HIF2a blocked the DMOG induced response of gremlin (HIF2a siRNA). Note that in the absence of DMOG siRNA did not significantly alter gremlin expression (non-targeting and siRNA targeting HIF2a). Values are shown as medians ±inter quartile ranges (n=6-7 per group) * indicates significant difference from matched normoxic group ($P<0.05$, Wilcoxon signed rank). **(B)** Gremlin 1 expression in human pulmonary artery smooth muscle cells was not significantly altered by two days of hypoxic exposure. Gremlin 1 mRNA expression (mean±SE) in PASMCs in response to 48 hours hypoxic exposure (*n*=4). Values are normalised to 18S RNA and expressed as fold-change relative to normoxic control.
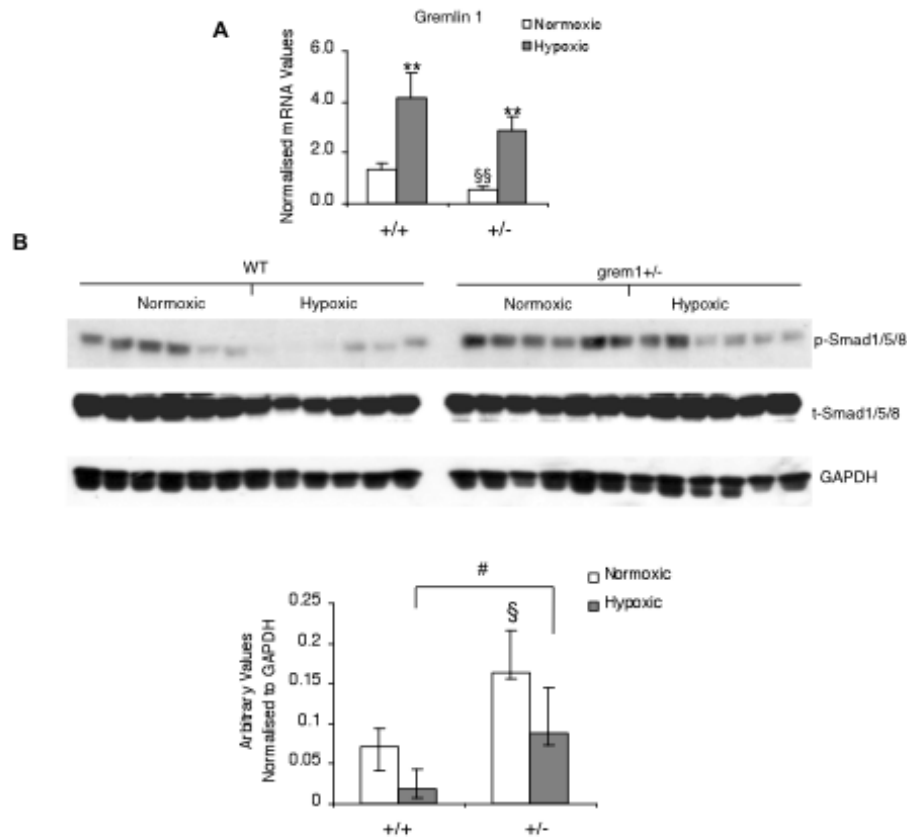
Supplemental Figure 7. Gremlin 1 inhibits basal Smad1/5/8 phosphorylation in human pulmonary microvascular endothelial cells. Treatment with recombinant gremlin 1 (2 micrograms/ml) for 1 hour significantly reduced basal Smad1/5/8 phosphorylation in these pulmonary endothelial cells. Densitometric analysis showed a statistically significant (**$P<0.01$) reduction in Smad1/5/8 phosphorylation following gremlin 1 treatment (median±IQR). Values were normalized to vehicle control value (n=6).
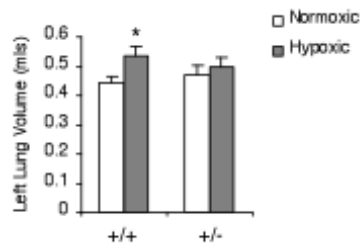
Supplemental Figure 8. BMP4 induces Smad1/5/8 in human pulmonary microvascular endothelial cells, which is similarly blocked by both recombinant gremlin 1 and hypoxia conditioned medium. Western blot showing Smad1/5/8 phosphorylation in pulmonary endothelial cells following treatment for one hour with vehicle, gremlin 1, recombinant BMP4, recombinant BMP4 together with recombinant gremlin 1, and BMP4 together with hypoxic conditioned medium respectively. Hypoxic conditioned medium was medium removed from pulmonary microvasclar endothelial cells that had been cultured in hypoxia for 48 hours. Densitometric analysis (median±IQR) showed that BMP4 treatment caused a significant increase in Smad1/5/8 phosphorylation whereas this action was not observed in the presence of gremlin 1 or hypoxia conditioned medium (n=6 per group). Gremlin 1 treatment alone reduced Smad1/5/8 phosphorylation significantly below that observed in the vehicle treated group. * and ** indicate significant difference from vehicle treatment (P<0.05 and <0.01 respectively).

Supplemental Figure 9. Polyclonal goat anti-gremlin antibody blocks gremlin function. Western blot showing that BMP2 treatment for 1 hour induced Smad1/5/8 phosphorylation in human pulmonary microvascular endothelial cells (lane 2) that was blocked by recombinant gremlin 1 (lane 3). Anti-gremlin antibody prevented the inhibitory action of gremlin 1 on BMP2-induced Smad 1/5/8 phosphorylation (lane 4).

Supplemental Figure 10. Gremlin 1 expression and BMP signaling in grem1^{+/-} and wild-type mice lungs. (**A**) Basal gremlin 1 mRNA expression (mean±SE) in grem1^{+/-} is significantly less than that in wild-type mice lungs and is upregulated in response to 2 days of hypoxic exposure in both groups (*n*=8). (**B**) Smad1/5/8 phosphorylation (median±IQR) is higher in normoxic grem1^{+/-} mice lungs than in normoxic wild-type mice lungs. Similarly Smad1/5/8 phosphorylation is higher in hypoxic grem1^{+/-} mice lungs than in normoxic wild-type mice lungs (*n*=6). [§] indicates significant difference between normoxic wild-type and normoxic grem1^{+/-} mice (*P*<0.05). [#] indicates significant difference between hypoxic wild-type and hypoxic grem1^{+/-} mice (*P*<0.05).

Supplemental Figure 11. The mean left lung volume (mean±SE) of the wild-type hypoxic mice was significantly larger than that of normoxic wild type mice. No significant difference was observed between the two grem1^{+/-} groups. Thus, grem1^{+/-} mice did not show the increased lung volume normally observed in response to chronic hypoxia [15, 21-23].

Supplemental References

1. Roxburgh SA, Kattla JJ, Curran SP, O'Meara YM, Pollock CA, Goldschmeding R, Godson C, Martin F, Brazil DP. Allelic Depletion of grem1 Attenuates Diabetic Kidney Disease. *Diabetes.* 2009;58(7):1641-1650.

2. Khokha MK, Hsu DR, Brunet LJ, Dionne MS, Harland RM. Gremlin is the BMP antagonist required for maintenance of Shh and Fgf signals during limb patterning. *Nat Genet.* 2003;34:303 - 307.

3. Costello CM, Howell K, Cahill E, McBryan J, Konigshoff M, Eickelberg O, Gaine S, Martin F, McLoughlin P. Lung-selective gene responses to alveolar hypoxia: potential role for the bone morphogenetic antagonist gremlin in pulmonary hypertension. *Am J Physiol Lung Cell Mol Physiol.* 2008;295(2):L272-284.

4. Kiyono M, Shibuya M. Inhibitory Smad transcription factors protect arterial endothelial cells from apoptosis induced by BMP4. *Oncogene.* 2006;25(54):7131-7137.

5. Star GP, Giovinazzo M, Langleben D. Effects of bone morphogenic proteins and transforming growth factor-beta on In-vitro production of endothelin-1 by human pulmonary microvascular endothelial cells. *Vascular Pharmacology.* 2009;50(1-2):45-50.

6. Zhang S, Fantozzi I, Tigno DD, Yi ES, Platoshyn O, Thistlethwaite PA, Kriett JM, Yung G, Rubin LJ, Yuan JXJ. Bone morphogenetic proteins induce apoptosis in human pulmonary vascular smooth muscle cells. *Am J Physiol Lung Cell Mol Physiol.* 2003;285(3):L740-754.

7.   Rothhammer T, Bataille F, Spruss T, Eissner G, Bosserhoff AK. Functional implication of BMP4 expression on angiogenesis in malignant melanoma. *Oncogene.* 2006;26(28):4158-4170.

8.   Maciel TT, Melo RS, Schor N, Campos AH. Gremlin promotes vascular smooth muscle cell proliferation and migration. *Journal of Molecular and Cellular Cardiology.* 2008;44(2):370-379.

9.   Morrell NW, Yang X, Upton PD, Jourdan KB, Morgan N, Sheares KK, Trembath RC. Altered Growth Responses of Pulmonary Artery Smooth Muscle Cells From Patients With Primary Pulmonary Hypertension to Transforming Growth Factor-{beta}1 and Bone Morphogenetic Proteins. *Circulation.* 2001;104(7):790-795.

10.   Suzuki Y, Montagne K, Nishihara A, Watabe T, Miyazono K. BMPs Promote Proliferation and Migration of Endothelial Cells via Stimulation of VEGF-A/VEGFR2 and Angiopoietin-1/Tie2 Signalling. *J Biochem.* 2008;143(2):199-206.

11.   Mitola S, Ravelli C, Moroni E, Salvi V, Leali D, Ballmer-Hofer K, Zammataro L, Presta M. Gremlin is a novel agonist of the major proangiogenic receptor VEGFR2. *Blood.* 2011;116(18):3677-3680.

12.   Wordinger RJ, Fleenor DL, Hellberg PE, Pang IH, Tovar TO, Zode GS, Fuller JA, Clark AF. Effects of TGF-beta2, BMP-4, and gremlin in the trabecular meshwork: implications for glaucoma. *Invest Ophthalmol Vis Sci.* 2007;48(3):1191-1200.

13.   Weissmann N, Akkayagil E, Quanz K, Schermuly RT, Ghofrani HA, Fink L, Hanze J, Rose F, Seeger W, Grimminger F. Basic features of hypoxic

pulmonary vasoconstriction in mice. *Respir Physiol Neurobiol.* 2004;139(2):191-202.

14. Cadogan E, Hopkins N, Giles S, Bannigan JG, Moynihan J, McLoughlin P. Enhanced expression of inducible nitric oxide synthase without vasodilator effect in chronically infected lungs. *Am J Physiol Lung Cell Mol Physiol.* 1999;277(3):L616-627.

15. Hyvelin J-M, Howell K, Nichol A, Costello CM, Preston RJ, McLoughlin P. Inhibition of Rho-Kinase Attenuates Hypoxia-Induced Angiogenesis in the Pulmonary Circulation. *Circ Res.* 2005;97(2):185-191.

16. von Bethmann AN, Brasch F, Nusing R, Vogt K, Volk HD, Muller KM, Wendel A, Uhlig S. Hyperventilation induces release of cytokines from perfused mouse lung. *American journal of respiratory and critical care medicine.* 1998;157(1):263-272.

17. Perk K, Frei YF, Herz A. Osmotic Fragility of Red Blood Cells of Young and Mature Domestic and Laboratory Animals. *Am J Vet Res.* 1964;25:1241-1248.

18. Howell K, Costello CM, Sands M, Dooley I, McLoughlin P. L-Arginine promotes angiogenesis in the chronically hypoxic lung: a novel mechanism ameliorating pulmonary hypertension. *Am J Physiol Lung Cell Mol Physiol.* 2009;296(6):L1042-1050.

19. Howell K, Preston RJ, McLoughlin P. Chronic hypoxia causes angiogenesis in addition to remodelling in the adult rat pulmonary circulation. *The Journal of Physiology.* 2003;547(1):133-145.

20. Ludbrook J. Multiple comparison procedures updated. *Clinical and experimental pharmacology & physiology.* 1998;25(12):1032-1037.

21. Cunningham EL, Brody JS, Jain BP. Lung growth induced by hypoxia. *J Appl Physiol.* 1974;37(3):362-366.

22. Howell K, Preston RJ, McLoughlin P. Chronic hypoxia causes angiogenesis in addition to remodelling in the adult rat pulmonary circulation. *J Physiol.* 2003;547(Pt 1):133-145.

23. Rabinovitch M, Gamble W, Nadas AS, Miettinen OS, Reid L. Rat pulmonary circulation after chronic hypoxia: hemodynamic and structural features. *Am J Physiol.* 1979;236(6):H818-827.